NJC

PAPER

View Article Online
View Journal | View Issue

Cite this: *New J. Chem.*, 2019, **43**, 17358

Aminonitrones as highly reactive bifunctional synthons. An expedient one-pot route to 5-amino-1,2,4-triazoles and 5-amino-1,2,4-oxadiazoles – potential antimicrobials targeting multi-drug resistant bacteria†

Mikhail V. Il'in, [a] Alexandra A. Sysoeva, [a] Dmitrii S. Bolotin, *[a] Alexander S. Novikov, [a] Vitalii V. Suslonov, [b] Elizaveta V. Rogacheva,[c] Liudmila A. Kraeva*[cd] and Vadim Yu. Kukushkin *[a]

The developed one-pot protocol to 5-amino-1,2,4-triazoles or 5-amino-1,2,4-oxadiazoles includes an interplay between aminonitrones $R^1C(NH_2){=}N^+(Me)O^-$ (R^1 = Alk, Ar, Het), isocyanides R^2NC (R^2 = Alk, Ar), Br_2, and hydrazines (for the triazoles) or hydroxylamine (for the oxadiazoles). This formally four-component reaction, involving aminonitrones, isocyanides, bromine, and *N*-nucleophiles, proceeds very rapidly under mild conditions (10 min, 20–25 °C), and is insensitive to moisture and air (in undried $CHCl_3$–MeOH, in air) and it gives the heterocyclic systems in good yields (up to 86%; 26 examples). The reaction scope includes aromatic-, heteroaromatic-, and aliphatic aminonitrones and also aliphatic- and aromatic isocyanides. Results of DFT calculations (M06-2X/6-311+G(d,p) level of theory) indicate that the *O*-nucleophilic center of bifunctional aminonitrones is more reactive than the *N* center; it first reacts with *in situ* generated R^2NCBr_2 to grant 2-methyl-1,2,4-oxadiazolium salts, which are then converted to the target heterocyclic systems upon treatment with hydrazines or hydroxylamine. The nature and strength of the intramolecular hydrogen bonds N–H···N and O–H···N, which significantly contribute to the total energies of different transition states and products of the nucleophilic substitution, were studied theoretically using the topological analysis of the electron density distribution within the framework of Bader's theory (QTAIM method). Several new 5-amino-3-aryl-1,2,4-triazoles and -1,2,4-oxadiazoles exhibit high antibacterial activity against multidrug-resistant bacteria strains such as *Staphylococcus aureus* and *Klebsiella pneumoniae* (MIC = 8 mg L^{-1}).

Received 2nd September 2019,
Accepted 16th October 2019

DOI: 10.1039/c9nj04529e

rsc.li/njc

Introduction

Oximes and, in particular, amidoximes are widely utilized precursors in organic and organometallic syntheses (see our reviews[1] and references therein). Our recent experimental and theoretical studies, which appeared concurrently with relevant works by Xu,[2] Merino[3] and coworkers, indicate that *O*-functionalization of (amid)oxime species *via* their nucleophilic addition to unsaturated species, which very often comprises the first step of their synthetic transformations, proceeds *via* initial tautomerization of (amid)-oxime to (amino)nitrones,[2–4] and the latter tautomeric form acts as an active nucleophile in these *O*-functionalizations (Scheme 1).[5] This finding prompted us to study the reactivity of such amidoxime congeners as aminonitrones to explore their potential as bifunctional nucleophilic organic synthons, particularly for the preparation of heterocyclic compounds.

Although aminonitrone species, which represent the nitrone tautomer "frozen" by *N*-alkylation (Scheme 1, right), can be easily obtained by the reaction of nitriles and *N*-substituted hydroxylamine (MeOH, 3 h, reflux; see the ESI†), their chemistry has received undeservedly little attention. Indeed, while the chemistry of amidoxime species is well developed, almost nothing is known

[a] *Institute of Chemistry, Saint Petersburg State University, Universitetskaya Nab., 7/9, Saint Petersburg, Russian Federation. E-mail: d.s.bolotin@spbu.ru, v.kukushkin@spbu.ru*
[b] *Center for X-ray Diffraction Studies, Saint Petersburg State University, Universitetskii Pr., 26, Saint Petersburg, Russian Federation*
[c] *Saint Petersburg Pasteur Institute, Mira Str., 14, Saint Petersburg, Russian Federation. E-mail: lykraeva@yandex.ru*
[d] *S. M. Kirov Military Medical Academy, Lebedeva Str., 6, Saint Petersburg, Russian Federation*

† Electronic supplementary information (ESI) available: Analytical and spectroscopy data for aminonitrones, syntheses and characterization of aminonitrones, syntheses and characterization of **1–26**, crystal data for **13** and **14**, the HRESI$^+$-MS, IR, ^{1}H and ^{13}C{^{1}H} NMR spectra of the aminonitrones and also **1–26**, and details of DFT calculations. CCDC 1901802 and 1901803. For ESI and crystallographic data in CIF or other electronic format see DOI: 10.1039/c9nj04529e

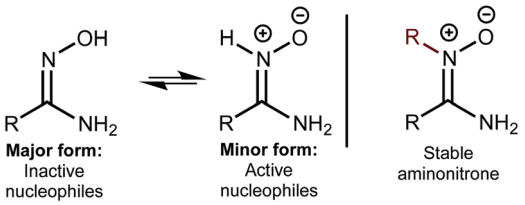

Scheme 1 Amidoxime–aminonitrone tautomerism.

about the reactions of structurally relevant aminonitrones. Aminonitrones can be oxidized to imino-nitroxides[6] and azo compounds,[7] or reduced to amidines.[7,8] These species can also be involved in heterocyclization to form imidazolones,[9] imidazoles,[9] 1,2,4-oxadiazolines,[9,10] 1,2,5-oxadiazin-4-ones,[8] and diazepines[8b] and they are useful reactants to achieve 2-substituted 1,2,4-oxadiazolium salts.[11] It is noteworthy in the context of this work that multi-component reactions based on aminonitrones are unknown.

We now report an expedient aminonitrone-based one-pot route to 5-amino-1,2,4-oxadiazoles and 5-amino-1,2,4-triazoles that can also be treated as a formally multicomponent reaction. A general overview of synthetic strategies leading to these 5-amino-substituted heterocyclic systems indicates a number of procedures, among which the most useful processes employ amidoxime or hydrazone species, respectively, and cyanamides (catalyzed by $ZnCl_2$; 80 °C, 26–54 h; Scheme 2, a),[12] carbodiimides (110 °C; 5–36 h; dry solvents; b),[13] or highly toxic cyanogen bromide (30 °C, overnight; c).[14] In addition, chlorooximes were introduced in the two-step 36 h-long procedure including isocyanides and hydroxylamine to yield 5-amino-1,2,4-oxadiazoles[15] (d).

Our aminonitrone-based approach has significant advantages over the known oxime-based synthetic procedures to yield 5-amino-1,2,4-oxadiazoles,[12–15] which also allows the synthesis of 5-amino-1,2,4-triazoles under the same mild conditions (e). Our interest in useful properties of novel systems, as well as the availability of facilities to assay their biological effects, led us to study the antibiotic properties of the obtained 5-amino-1,2,4-triazoles and 5-amino-1,2,4-oxadiazoles. Antibacterial activity has previously been studied for a wide range of 1,2,4-triazoles[16] and 1,2,4-oxadiazoles,[17] but it has never been verified for their 5-amino-derivatives; the latter heterocyclic systems were previously considered only from the viewpoint of their application in materials chemistry.[14b,18]

Results and discussion

Aminonitrone-based synthesis of 5-amino-1,2,4-triazoles and 5-amino-1,2,4-oxadiazoles

Consequent addition of dibromine, the aminonitrone $R^1C(NH_2)$═$N^+(Me)O^-$, and any of the bifunctional nucleophiles H_2NXH

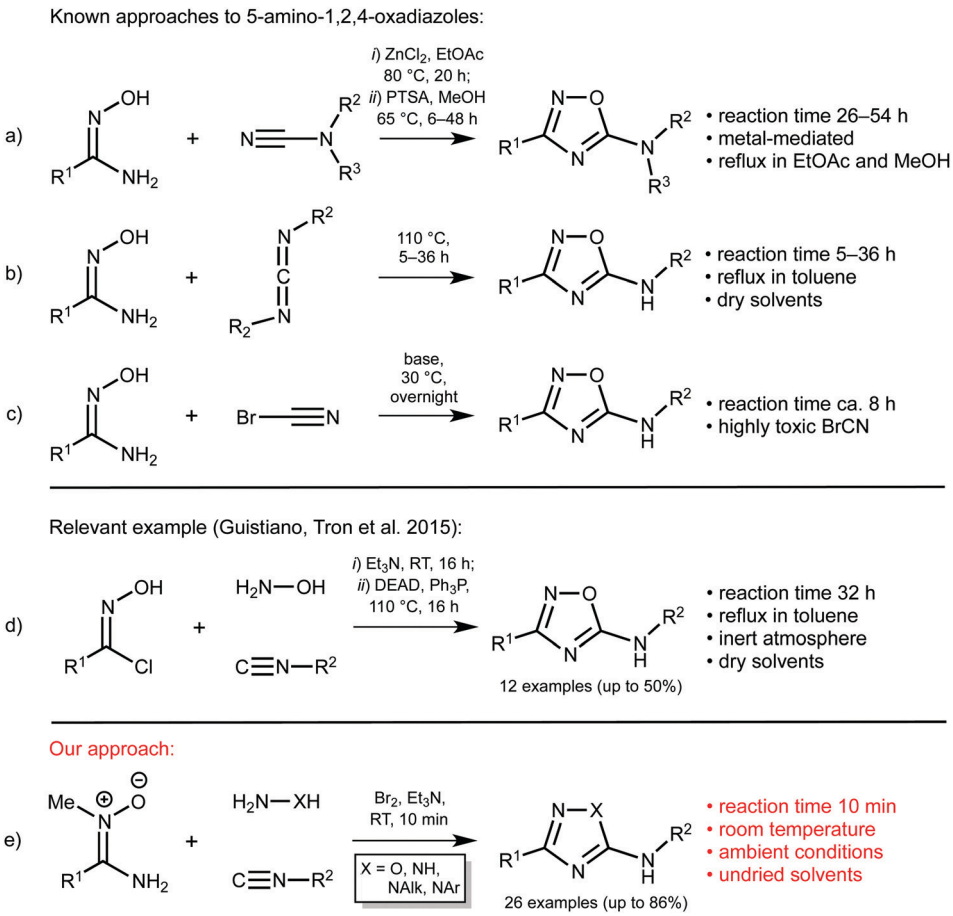

Scheme 2 Reported amidoxime-based and novel aminonitrone-based approaches to 5-aminoheterocycles.

(hydroxylamine; hydrazine, phenyl- and benzylhydrazines were taken as model mono-substituted hydrazines) to a solution of R^2NC in $CHCl_3$ at RT for 10 min resulted in the generation of 5-R(H)N-1,2,4-oxadiazoles (**15–26**) or 5-R(H)N-1,2,4-triazoles (**1–14**), which, after work-up, were isolated in up to 86% yields (Scheme 3). Heterocycles **2–14**, **16–17**, and **19–22** were characterized by HRESI$^+$-MS, IR, and ^{1}H- and $^{13}C\{^1H\}$ NMR spectroscopies. Compounds **1**,[11] **15**,[11] **18**,[19] and **23**[15] were previously reported and they were identified by comparison of their NMR spectra with the reported spectral data and also by measuring their HRESI$^+$-mass spectra. 1-Substituted triazoles **13** and **14** were additionally characterized by single-crystal XRD (see the ESI†).

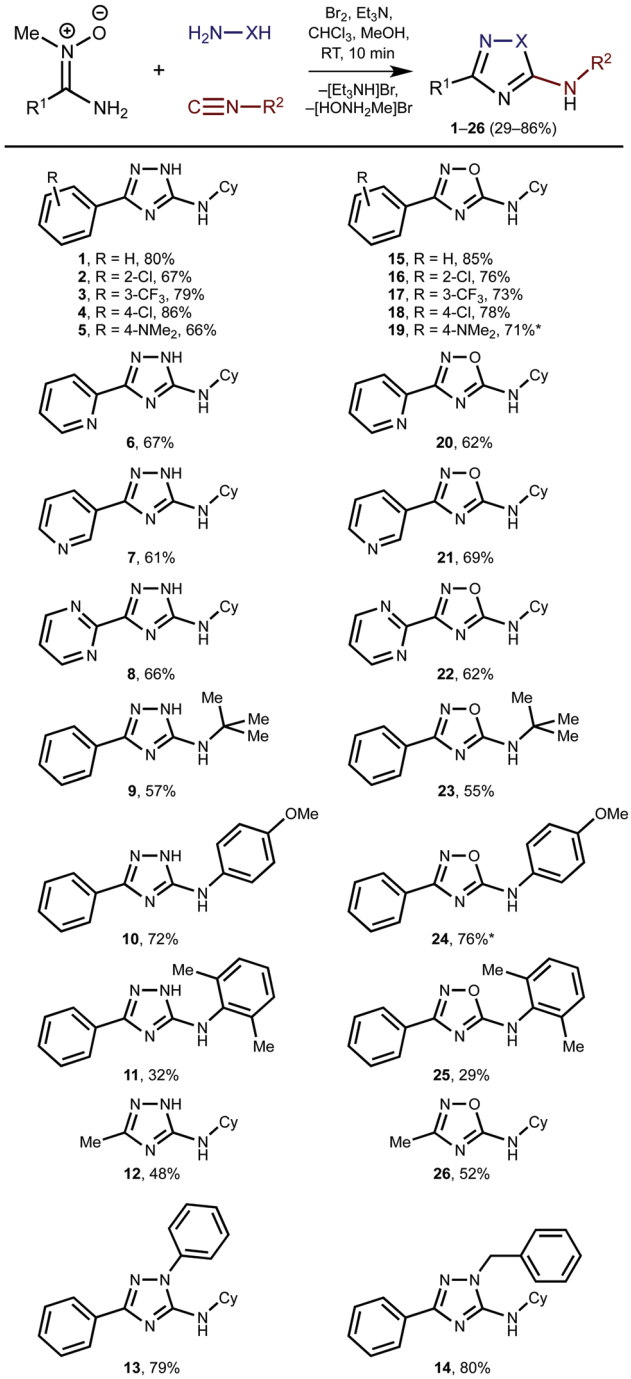

Scheme 3 Preparation of 5-amino-1,2,4-triazoles and 5-amino-1,2,4-oxadiazoles. Reagent ratios: aminonitrone (1 equiv.), isocyanide (1.2 equiv.), H_2NX (1.5 equiv.), Br_2 (1.2 equiv.), and Et_3N (1 equiv.). * Combined yields for obtained mixtures of 5-amino and 3-amino regioisomers are represented (**19**: ~10 : 1; **24**: ~20 : 1, respectively).

For the aromatic aminonitrones the reaction typically proceeded in higher yields than that for aliphatic substrates [R^2 = Cy; 61–86% (R^1 = Ar; **1–8** and **15–22**) *vs.* 48 and 52% (R^1 = Me; **12** and **26**)]. Sterically hindered R^2 significantly reduced the yield of heterocycles and, thus, isocyanides XylNC and ^{t}BuNC gave **9**, **11**, **23**, and **25** in 29–57% yields. The nature of the bifunctional nucleophile had almost no effect on the yield of heterocycles and **1**, **13**, **14**, and **15** (R^1 = Ph; R^2 = Cy; X = NH, NPh, NBn, and O, respectively) were isolated in similar yields (79–85%). Electronic effects of substituents in aromatic aminonitrones also had no significant effect on the yield of heterocycles. It is important to note that traces of water and dioxygen did not affect the yields of **1–26**; employment of dry solvents and/or an inert atmosphere (under Ar) did not improve the yields.

For the first step of the reactions (generation of 1,2,4-oxadiazolium salts; see below), weak donor solvents should be used. We found no significant effect on the yields of **1–26** upon the utilization of $CHCl_3$, CH_2Cl_2, and $ClCH_2CH_2Cl$, whereas in more donating Me_2CO, Me_2SO, and DMF, the yields, in general, were by 15–30% lower. When the first step of the reaction was conducted in MeOH or EtOH, the treatment led to a spectrum of by-products and finally gave **1–26** in ^{1}H NMR yields less than 35%. Utilization of MeOH or EtOH is possible on the second step of the reaction, when the formed 1,2,4-oxadiazolium salt reacts with H_2NX. Increasing the molar ratio between RNC and Br_2 relative to the aminonitrone to (1.5) : (1.5) : 1 did not lead to an appropriate increase in the yields of **1–26**, whereas the decrease to 1 : 1 : 1 resulted in yield reduction by 10–15%, compared to the reactions performed with the (1.2) : (1.2) : 1 molar ratio. Increasing the ratio of Et_3N : aminonitrone from 1 : 1 to (1.5) : 1 and then to 2 : 1 led to a gradual decrease of the yields of **1–26** by *ca.* 5–10%, whereas the decrease of the ratio resulted in substantial yield reduction.

Regioselectivity of the reactions with unsymmetric nucleophiles

When the unsymmetric bifunctional nucleophiles (H_2NX; X = NHPh, NHBn, OH) were applied, in each case, generation of a mixture of regioisomers was observed (Fig. 1).

The reactions including phenyl- and benzylhydrazines (for **13** and **14**, respectively) proceed to give mixtures of the 5-amino-1,2,4-triazole (major) and 3-amino-1,2,4-triazole (minor) forms in 95 : 5 and 90 : 10 molar ratios, correspondingly (based on ^{1}H NMR and GC-MS monitoring). Similarly, when H_2NOH was employed for the preparation of **15–26**, in each case a regioisomeric mixture of 5-amino-1,2,4-oxadiazole (major) and 3-amino-1,2,4-oxadiazole (minor) is generated in an approximately 95 : 5 molar ratio (except **19**, where this molar ratio was 87 : 13). In all cases (except **19** and **24**), the major 5-amino isomer

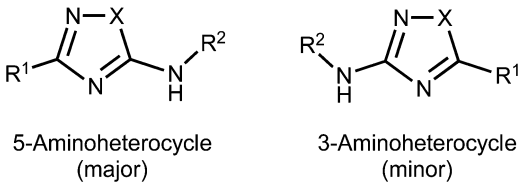

Fig. 1 Two regioisomers of **13–26**.

was isolated from the reaction mixture as a pure compound by column chromatography. In the cases of **19** and **24**, the major 5-amino isomer was contaminated with traces of the minor 3-amino isomer; close retention times on silica gel—that remained almost the same even upon substantial variation of eluent systems—did not lead to complete separation. Lower selectivity of the reaction in the case of **19** could be explained in terms of the +*M* effect of the NMe_2 group leading to decreased electrophilicity of the C-3 atom. Variation in solvents (for **13** and **14**; $CHCl_3$, CH_2Cl_2, and $ClCH_2CH_2Cl$) or solvent mixtures (for **19**; $CHCl_3$, CH_2Cl_2, $ClCH_2CH_2Cl$ and MeOH, or EtOH) did not affect significantly the molar ratios of the regioisomers.

Insights into the reactivity of aminonitrones: a plausible mechanism of the reaction

The overall reaction route includes three principal steps. The first step is the initial generation of carbonimidic dibromides $Br_2C{=}NR^2$ from isocyanides and dibromine (Scheme 4, a).[20] Isocyanide dihalides are known to react with a series of nucleophiles,[20a,21] including bifunctional nucleophiles[22] to give heterocyclic systems. Accordingly, in the next step, $Br_2C{=}NR^2$ reacts with aminonitrone to give electrophilically activated 5-amino-2-methyl-1,2,4-oxadiazolium salt *via* two consequent nucleophilic substitutions (b).[11] Although uncharged 1,2,4-oxadiazoles are typically inactive toward nucleophilic attack, these heterocyclic systems bearing strong electron-withdrawing perfluoroalkyl groups undergo ANRORC rearrangements,[23] which usually proceed for electron-deficient aromatic systems.[24] Positive charge on the aromatic system of a generated 2-methyl-1,2,4-oxadiazolium salt facilitates the nucleophilic attack by H_2NX to grant the 1,2,4-triazole or 1,2,4-oxadiazole systems (**1–26**) *via* the ANRORC route (c).

In order to extend the existing knowledge on the reactivity of aminonitrone species, we focused our attention on the first step (*a*) and conducted an additional computational study. As can be inferred from our previous work,[25] aminonitrone species exist in two tautomeric forms, *viz.* the major aminonitrone form featuring the *O*-nucleophilic site (Scheme 5, **A**) and the minor iminohydroxamic acid form featuring the *N*-nucleophilic site (**B**). The aminonitrone species **A** can form *O*-iminoacyl aminonitrones **D**, whereas the iminohydroxamic species **B** can form *N*-iminoacylated intermediates **E**. Both **D** and **E** may further undergo heterocyclization in a basic medium leading to the same product (**F**). Thus, which site of the starting bifunctional nucleophile reacts first in the sequence of the two nucleophilic substitutions was an open question.

Results of DFT calculations (M06-2X/6-311+G(d,p) level of theory, for details see the ESI†) performed for exact pairs of the reactants (R^1 = Ph; R^2 = Cy) reveal that (i) isomer **A** is thermodynamically more favorable than **B** (by 0.9 kcal mol^{-1} in terms

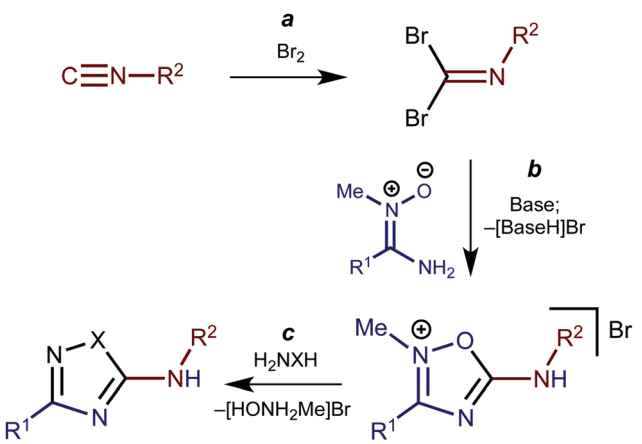

Scheme 4 A plausible mechanism of the reaction.

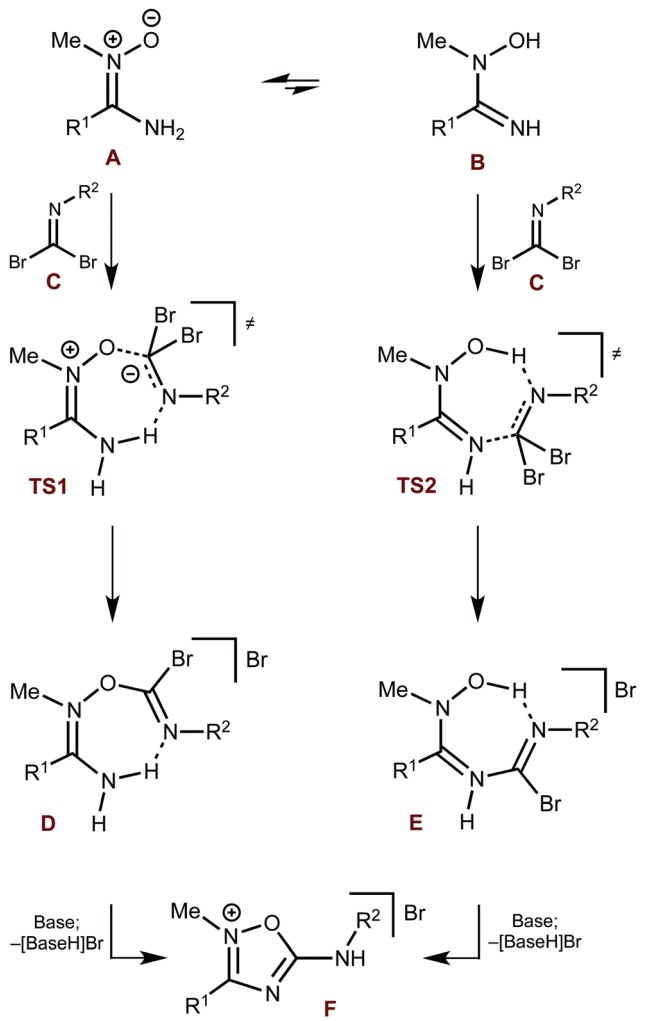

Scheme 5 Plausible routes for the nucleophilic substitutions at an isocyanide dibromide by an aminonitrone.

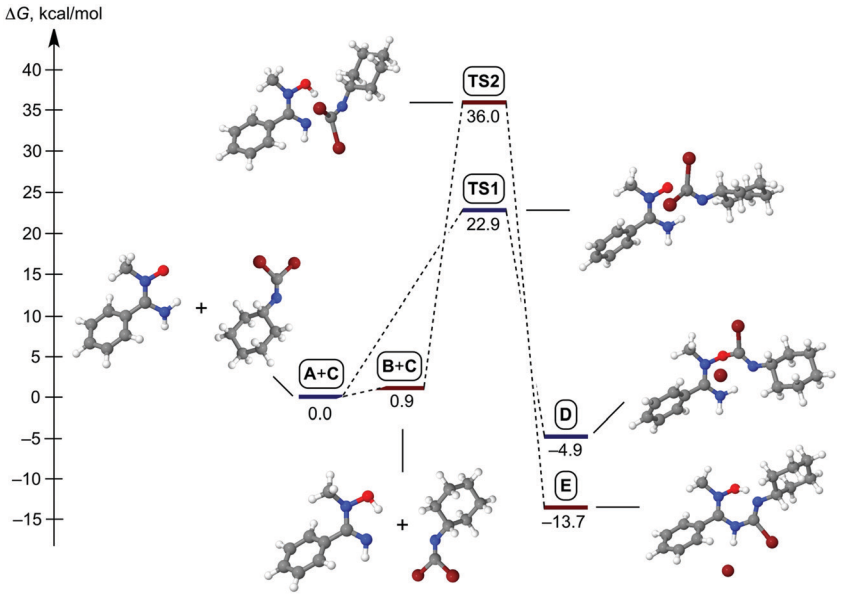

Scheme 6 Energy profiles for plausible routes of the nucleophilic substitution.

of Gibbs free energies; Scheme 6), (ii) the reaction pathway **A** + **C** → **D** is more kinetically favorable than the reaction pathway **B** + **C** → **E** (by 12.2 kcal mol^{-1} in terms of Gibbs free energies of activation), and (iii) the formation of **E** is more thermodynamically profitable than the formation of **D** (by 8.8 kcal mol^{-1} in terms of Gibbs free energies of reaction). Based on the theoretical calculations and experimental observations it can be concluded that the aminonitrone species are first acylated *via* the O atom. Because of the relatively high activation energy, alternative *N*-acylation at room temperature is hardly possible.

Because the suggested transition states and the iminoacylated intermediates feature intramolecular hydrogen bonds, which may significantly contribute to their total energy, we have estimated the strength of the intramolecular hydrogen bonds N–H···N and O–H···N in optimized equilibrium model structures of transition states and products of nucleophilic substitution using the topological analysis of the electron density distribution within the framework of Bader's theory (QTAIM method).[26] This approach has already been successfully used by us upon studies of different hydrogen bonds in various organic,[27] organometallic,[28] and coordination compounds,[29] as well as for the investigation of properties of transition states in cycloaddition reactions.[30] The results are summarized in Table 5S (ESI†).

The QTAIM analysis performed for the optimized equilibrium model structures of transition states and products of nucleophilic substitution demonstrates the presence of appropriate bond critical points (3, −1) (BCPs; Fig. 141S and 142S, ESI†) for intramolecular hydrogen bonding N–H···N and O–H···N in all cases (Table 5S, ESI†). The low magnitude of the electron density (0.017–0.019 a.u.), positive values of the Laplacian (0.064–0.067 a.u.), and very close to zero positive energy density in BCPs for N–H···N contacts in **TS1** and **D** and O–H···N contact in **TS2** as well as negligible Wiberg bond indices (0.01–0.02) for these interactions are typical for purely noncovalent weak hydrogen bonds, whereas analysis of the properties of O–H···N contact in **E** (*viz.* relatively large magnitude of the electron density and negative energy density in appropriate BCP, $G(\mathbf{r}) \ll |V(\mathbf{r})|$, a large value of Wiberg bond index) suggests that this hydrogen bond has a large degree of covalent components and it is relatively strong (Table 5S, ESI†). Thus, higher thermodynamic stability of this isomer compared with **D** may be accounted for by the presence of the strong intramolecular O–H···N hydrogen bond in **E**.

Antibacterial activity of 5-amino-1,2,4-triazoles and 5-amino-1,2,4-oxadiazoles

We studied antibacterial activity of aminoheterocycles **1–26**, as well as the activity of all starting aminonitrones, against bacterial species from the ESKAPE group. It is important to note that the widespread use of antibiotics led to a significant increase of the resistance of bacteria that circulate not only in the hospital environment, but also in outpatient settings.[31] The greatest danger is posed by bacterial species from the ESKAPE group (*i.e. Enterococcus faecium, Staphylococcus aureus, Klebsiella pneumoniae, Acinetobacter baumannii, Pseudomonas aeruginosa* and *Enterobacter* species). They are often multi-resistant to antibiotics; according to ref. 32, the proportion of resistant strains can even reach 95%. The greatest resistance to antibiotics is noted in strains *S. aureus* and *K. pneumonia*; the former uses a wide range of resistance mechanisms. Therefore, new small molecules that affect cell viability have recently been developed.[33]

In our antibacterial experiments, initially, compounds **1–26** were tested by the disk diffusion method to choose the most active species. Starting aminonitrones generally exhibited no significant activity toward the studied bacterial strains, whereas selected heterocyclic compounds were then studied by the minimum inhibitory concentration (MIC) method according to the international standard EUCAST 2018 (Version 8.1) (Table 1).

Table 1 Minimum inhibitory concentrations (mg L^{-1}) of the selected 1,2,4-oxadiazoles and 1,2,4-triazoles toward ESKAPE bacterial pathogens

No.	*Enterococcus faecalis*	*Staphylococcus aureus*	*Klebsiella pneumoniae*	*Acinetobacter baumannii*	*Pseudomonas aeruginosa*	*Enterobacter cloacae*
2	>300	8	8	75	300	>300
3	75	8	8	75	300	32
5	>300	8	150	8	300	>300
6	8	8	75	150	300	32
8	8	75	8	75	150	300
10	75	8	8	8	300	300
12	>300	>300	8	75	75	300
16	150	8	8	8	150	300
Ciprofloxacin	0.3	2.5	0.6	1.25	1.25	0.6

As it can be inferred from the obtained experimental data, the selected compounds have encouraging activity against *S. aureus* and *K. pneumoniae*. Some of our compounds also exhibit activity against *E. faecalis* (**6** and **8**) and *A. baumannii* (**5**, **10**, **16**), whereas no significant activity was observed against *P. aeruginosa* and *E. cloacae*.

On the one hand, **2**, **3**, **5**, **6**, **10**, and **16** demonstrated MIC 8 mg L^{-1} toward *S. aureus*, which is similar to the MIC values for *Chloramphenicol* and *Amikacin* and it is only twice higher than that of such very strong antibiotics as *Linezolid* and *Vancomicin*. The activity of the aminoheterocycles toward *S. aureus* is in the range between the activity of 1-*H*-5-alkylthio-1,2,4-triazoles[34] and 5-alkylthio-1,2,4-triazoles bearing ciprofloxacin moieties[35] and lies in the same activity interval as 3,5-diaryl-1,2,4-oxadiazoles.[36] On the other hand, compounds **2**, **3**, **8**, **10**, **12**, and **16** exhibited MIC 8 mg L^{-1} against *K. pneumoniae*, which is similar to the activity of *Cefuroxime*, *Chloramphenicol*, and *Amikacin*. This activity is comparable with the activity of 5-alkyl-3-aryl-1,2,4-oxadiazoles,[37] but lower than that of ciprofloxacin-derived 5-alkylthio-1,2,4-triazoles.[35a]

Currently no solid ''structure–activity'' correlations for the tested compounds were observed. It is noteworthy, however, that the antibacterially active compounds are almost exclusively represented by the 1,2,4-triazoles and only one example of a 1,2,4-oxadiazole (**16**) manifests this type of activity. Furthermore, antibacterial studies could also be focused on the *ortho*-substituted 3-phenyl-1,2,4-oxadiazoles and -triazoles, wherein both (**16** and **2**, respectively) displayed high activities against *S. aureus* and *K. pneumoniae*.

Concluding remarks

The results of this work can be considered from at least three perspectives. First, we found an efficient synthetic utilization of aminonitrones, whose synthetic potential is practically uncovered. The developed one-pot reaction that can be treated as a formally four-component reaction comprises a facile and convenient one-pot route to 5-amino-1,2,4-triazoles and 5-amino-1,2,4-oxadiazoles; this synthesis is based on commercially available and/or easily accessible precursors. The reaction proceeds very rapidly under mild conditions (at RT for only 10 min) in undried solvents in air. The suggested method is applicable for the preparation of both the 3-alkyl- or 3-aryl heterocycles, as well as for the generation of not only 1-*H*-, but also 1-alkyl- and 1-aryl-1,2,4-triazoles.

Second, based on our experimental data and theoretical calculations one can suggest that although aminonitrones possess two nucleophilic sites featured by the aminonitrone and iminohydroxamic acid tautomers, the most reactive is the *O*-nucleophilic aminonitrone form. This observation shed light on the reactivity patterns of aminonitrone species and this adds to the existing knowledge on the reactivity of aminonitrones. Our studies also provide additional information on the reactivity of relevant amidoximes, whose reactions are generally determined by the reactivity of their minor tautomeric aminonitrone forms.[3,4] Results of DFT calculations and topological analysis of the electron density distribution within the framework of Bader's theory (QTAIM method) reveal that intramolecular hydrogen bonds N–H···N and O–H···N may significantly affect the thermodynamic stability of the formed iminoacylated intermediates.

Third, while the efficacy of compounds **2**, **3**, **8**, **10**, **12**, and **16** against *S. aureus* and *K. pneumoniae* in our experiments (MIC = 8 mg L^{-1}) is comparable with that of the known antibiotics, they represent a novel type of antimicrobials, to which bacterial populations have not yet evolved resistance. In light of the worldwide crisis of antimicrobial drug resistance, the clinical efficacy of our heterocycles may prove to be much higher than that of long-used antibiotics. These considerations stimulate our interest in the antibacterial properties of 5-amino-aminoheterocyclic systems, and further investigations are in progress in our group.

Experimental

Materials and instrumentation

Solvents, nitriles, *N*-methylhydroxylamine hydrochloride, isocyanides, bromine, triethylamine, hydroxylamine hydrochloride, hydrazine hydrate, and phenyl- and benzylhydrazine were obtained from commercial sources and used as received. All syntheses were conducted in air. Chromatographic separation was carried out on Macherey-Nagel silica gel 60 M (0.063–0.2 mm). Analytical TLC was performed on unmodified Merck ready-to-use plates (TLC silica gel 60 F254) with UV detection. Melting points were measured on a Stuart SMP30 apparatus in capillaries and are not corrected. Electrospray ionization mass-spectra were obtained on a Bruker maXis spectrometer

equipped with an electrospray ionization (ESI) source. The instrument was operated in positive ion mode using an *m*/*z* range 50–1200. The nebulizer gas flow was 1.0 bar and the drying gas flow 4.0 L min^{-1}. For HRESI$^+$, the studied compounds were dissolved in MeOH. Infrared spectra (4000–400 cm^{-1}) were recorded on a Shimadzu IR Prestige-21 instrument in KBr pellets. ^1H, $^{13}C\{^1H\}$ NMR spectra were measured on a Bruker Avance 400 spectrometer in $CDCl_3$, $(CD_3)_2SO$, and CD_3OD at ambient temperature; the residual solvent signal was used as the internal standard.

X-ray structure determinations

Single-crystal X-ray diffraction experiments were carried out using Agilent Technologies "SuperNova" and "Xcalibur" diffractometers with monochromated CuKα (**14**) and MoKα (**13**) radiation, respectively. The crystals were kept at 130(2) and 100(2) K during all data collection. The structures were solved by the Superflip[38] (**13**) and ShelXT[39] (**14**) structure solution programs using Charge Flipping and Intrinsic Phasing methods, respectively, and refined by means of the ShelXL[40] program, incorporated in the OLEX2[41] program package. CCDC numbers 1901802 and 1901803 contain the supplementary crystallographic data for this paper.

Details of DFT calculations

The full geometry optimization of all model structures has been carried out at the DFT level of theory using the M06-2X functional with 54% Hartree–Fock exchange[42] with the help of the Gaussian-09[43] program package. The standard 6-311+G(d,p) basis sets were used for all atoms. No symmetry restrictions have been applied during the geometry optimization procedure. The solvent effects were taken into account using the SMD continuum solvation model by Truhlar and coworkers[44] with chloroform as a solvent. The Hessian matrices were calculated analytically for all optimized model structures to prove the location of correct minima or saddle points (transition state) on the potential energy surface (no imaginary frequencies or only one imaginary frequency, respectively) and to estimate the thermodynamic parameters, the latter being calculated at 25 °C (Tables 1S–2S, ESI†). The nature of the transition states was studied by the analysis of vectors associated with the imaginary frequency and by the calculation of intrinsic reaction coordinates (IRC) using the Gonzalez–Schlegel method.[45] The topological analysis of the electron density distribution with the help of the atoms in molecules (QTAIM) method developed by Bader[26] has been performed by using the Multiwfn program.[46] The Wiberg bond indices were computed by using the Natural Bond Orbital (NBO) partitioning scheme.[47] The Cartesian atomic coordinates for all optimized equilibrium model structures are presented in Table 3S (ESI†).

Syntheses of 1–26

A solution of Br_2 (1.2 mmol) in $CHCl_3$ (1 mL) was dropwise added (1 min) to a stirred solution of isocyanide (1.2 mmol) in $CHCl_3$ (1 mL) placed in a 10 mL round-bottomed flask. The mixture was kept under stirring for 2 min at RT in air and then an aminonitrone (1.0 mmol) and Et_3N (1.0 mmol) were added to the reaction mixture. After 3 min a solution of hydrazine (for **1–12**; 1.5 mmol) or hydroxylamine (for **15–26**; 1.5 mmol) in MeOH (3 mL) was added. For **13** and **14** liquid phenyl- or benzylhydrazine, respectively, was added without additional dissolution in MeOH. The reaction mixture was left for an additional 4 min at RT and then the solvent was evaporated *in vacuo* at 40 °C. Final substrates **1–26** were isolated *via* column chromatography (for each product, the eluent is specified in characterization).

Analytical and spectroscopy data for 1–26

Compounds **1–26** were characterized by HRESI$^+$-MS, IR, and ^1H- and $^{13}C\{^1H\}$ NMR spectroscopies. In addition, **13** and **14** were studied by single-crystal X-ray diffraction.

The HRESI$^+$ mass-spectra of **1–26** exhibit peaks corresponding to the quasi-ions $[M + H]^+$, $[M + Na]^+$, $[2M + H]^+$, and $[2M + Na]^+$. The IR spectra of **1–26** display one to three weak-to-medium bands in the range of 3438–3058 cm^{-1}, which were attributed to the N–H stretches. Weak-to-strong bands at 3098–2726 cm^{-1} were assigned to the ν(C–H). The IR spectra of **1–26** display one or two medium-to-very-strong bands in the range of 1676–1530 cm^{-1}, which were attributed to the C=N stretches.

The ^1H NMR spectra of **1–12** expectedly display two sets of signals from 1*H*- and 2*H*-1,2,4-triazole tautomers, which are commonly observed for 5-amino-1,2,4-triazole derivatives.[12a,48] Thus, **1–7** and **9–12** display a broad signal of N–N*H* in the region of δ 13.61–11.76 (no signal of the NH was observed for **8**, which could be explained in terms of fast exchange with water). The ^1H NMR spectra of **2**, **5**, **6**, and **9–11** recorded in $(CD_3)_2SO$ reveal two signal sets of N–N*H* in the triazole ring and N*H* in the amino-group. The ^1H NMR spectra of **23**, **25** and **26** measured in $CDCl_3$ display one set of signals (δ 1.45–1.35) of the methyl moiety, whereas the spectrum of **19** and **24** displays two signals of the CH_3 moiety at δ 3.04, 3.07 and 3.76, 3.73 respectively, which indicates the availability of two isomeric forms of these compounds around the N–O bond in the 1,2,4-oxadiazolium ring (similarly there is two sets of signals in other areas). In the ^1H NMR spectrum of **3**, **4**, **6**, and **12**, the C*H*NH signals overlap with the residual signals of water. The $^{13}C\{^1H\}$ NMR spectra of **13–18**, **20–23**, **25**, and **26** recorded in $CDCl_3$ exhibit one set of signals of the C atoms of the 1,2,4-oxadiazolium ring in the region of δ 171.22–152.95, whereas the spectra of **19** and **24** display two sets of signals. This is coherent with the ^1H NMR data indicating the availability of the two isomeric forms.

Conflicts of interest

There are no conflicts to declare.

Acknowledgements

This work is a combination of two projects of the Russian Foundation for Basic Research: the synthetic part and the study of antibacterial activity were supported by grant 18-33-20012, whereas quantum chemical calculations by grant 19-03-00044. Physicochemical studies were performed at the Center for

Magnetic Resonance, the Center for X-ray Diffraction Studies, and the Center for Chemical Analysis and Materials Research (all belonging to Saint Petersburg State University).

References

1 (*a*) D. S. Bolotin, N. A. Bokach, M. Y. Demakova and V. Y. Kukushkin, *Chem. Rev.*, 2017, **117**, 13039–13122; (*b*) D. S. Bolotin, N. A. Bokach and V. Y. Kukushkin, *Coord. Chem. Rev.*, 2016, **313**, 62–93.

2 W. X. Liu, C. Zhang, H. Zhang, N. Zhao, Z. X. Yu and J. Xu, *J. Am. Chem. Soc.*, 2017, **139**, 8678–8684.

3 D. Roca-López, A. Darù, T. Tejero and P. Merino, *RSC Adv.*, 2016, **6**, 22161–22173.

4 D. S. Bolotin, V. K. Burianova, A. S. Novikov, M. Y. Demakova, C. Pretorius, P. P. Mokololokolo, A. Roodt, N. A. Bokach, V. V. Suslonov, A. P. Zhdanov, K. Y. Zhizhin, N. T. Kuznetsov and V. Y. Kukushkin, *Organometallics*, 2016, **35**, 3612–3623.

5 D. S. Bolotin, M. V. Il'in, A. S. Novikov, N. A. Bokach, V. V. Suslonov and V. Y. Kukushkin, *New J. Chem.*, 2017, **41**, 1940–1952.

6 H. G. Aurich and J. Trosken, *Chem. Ber.*, 1972, **105**, 1216–1223.

7 A. R. Forrester and R. H. Thomson, *J. Chem. Soc.*, 1965, 1224–1231.

8 (*a*) B. Trzewik, D. Cież, M. Hodorowicz and K. Stadnicka, *Synthesis*, 2008, 2977–2985; (*b*) B. Trzewik, T. Seidler, E. Brocławik and K. Stadnicka, *New J. Chem.*, 2010, **34**, 2220–2228.

9 P. S. Branco, S. Prabhakar, A. M. Lobof and D. J. Williams, *Tetrahedron*, 1992, **48**, 6335–6360.

10 (*a*) C. Z. Dong, A. Ahamada-Himidi, S. Plocki, D. Aoun, M. Touaibia, N. Meddad-Bel Habich, J. Huet, C. Redeuilh, J. E. Ombetta, J. J. Godfroid, F. Massicot and F. Heymans, *Bioorg. Med. Chem.*, 2005, **13**, 1989–2007; (*b*) B. N. Naidu and M. E. Sorenson, *Org. Lett.*, 2005, **7**, 1391–1393.

11 M. V. Il'in, D. S. Bolotin, V. V. Suslonov and V. Y. Kukushkin, *New J. Chem.*, 2018, **42**, 9373–9376.

12 (*a*) S. N. Yunusova, D. S. Bolotin, V. V. Suslonov, M. A. Vovk, P. M. Tolstoy and V. Y. Kukushkin, *ACS Omega*, 2018, **3**, 7224–7234; (*b*) D. S. Bolotin, K. I. Kulish, N. A. Bokach, G. L. Starova, V. V. Gurzhiy and V. Y. Kukushkin, *Inorg. Chem.*, 2014, **53**, 10312–10324.

13 (*a*) M. Ispikoudi, M. Amvrazis, C. Kontogiorgis, A. E. Koumbis, K. E. Litinas, D. Hadjipavlou-Litina and K. C. Fylaktakidou, *Eur. J. Med. Chem.*, 2010, **45**, 5635–5645; (*b*) M. Krasavin, K. A. Rufanov, A. V. Sosnov, R. Karapetian, E. Godovykh, O. Soldatkina, Y. Lavrovsky and A. A. Gakh, *Chem. Cent. J.*, 2010, **4**, 1–5; (*c*) W.-P. Yen, F.-C. Kung and F. F. Wong, *Eur. J. Org. Chem.*, 2016, 2328–2335.

14 (*a*) Y. Qu, Q. Zeng, J. Wang, Q. Ma, H. Li, H. Li and G. Yang, *Chem. – Eur. J.*, 2016, **22**, 12527–12532; (*b*) Q. Wang, Y. Shao and M. Lu, *Cryst. Growth Des.*, 2018, **18**, 6150–6154.

15 V. Mercalli, A. Massarotti, M. Varese, M. Giustiniano, F. Meneghetti, E. Novellino and G. C. Tron, *J. Org. Chem.*, 2015, **80**, 9652–9661.

16 C.-H. Zhou and Y. Wang, *Curr. Med. Chem.*, 2012, **19**, 239–280.

17 A. Pace and P. Pierro, *Org. Biomol. Chem.*, 2009, **7**, 4337–4348.

18 (*a*) R. Vaidhyanathan, S. S. Iremonger, G. K. Shimizu, P. G. Boyd, S. Alavi and T. K. Woo, *Angew. Chem., Int. Ed.*, 2012, **51**, 1826–1829; (*b*) R. B. Lin, D. Chen, Y. Y. Lin, J. P. Zhang and X. M. Chen, *Inorg. Chem.*, 2012, **51**, 9950–9955; (*c*) K.-J. Chen, R.-B. Lin, P.-Q. Liao, C.-T. He, J.-B. Lin, W. Xue, Y.-B. Zhang, J.-P. Zhang and X.-M. Chen, *Cryst. Growth Des.*, 2013, **13**, 2118–2123; (*d*) B. Liu, J. Shi, K.-F. Yue, D.-S. Li and Y.-Y. Wang, *Cryst. Growth Des.*, 2014, **14**, 2003–2008; (*e*) B. Liu, R. Zhao, K. Yue, J. Shi, Y. Yu and Y. Wang, *Dalton Trans.*, 2013, **42**, 13990–13996; (*f*) B. Liu, R. Zhao, G. Yang, L. Hou, Y.-Y. Wang and Q.-Z. Shi, *CrystEngComm*, 2013, **15**, 2057–2060; (*g*) J. Gao, N. Wang, X. Xiong, C. Chen, W. Xie, X. Ran, Y. Long, S. Yue and Y. Liu, *CrystEngComm*, 2013, **15**, 3261–3270; (*h*) Y. Q. Jiao, H. Y. Zang, X. L. Wang, E. L. Zhou, B. Q. Song, C. G. Wang, K. Z. Shao and Z. M. Su, *Chem. Commun.*, 2015, **51**, 11313–11316; (*i*) M. Finšgar, *Corros. Sci.*, 2013, **77**, 350–359; (*j*) E.-S. M. Sherif, *J. Ind. Eng. Chem.*, 2013, **19**, 1884–1889; (*k*) L. Guo, W. Dong and S. Zhang, *RSC Adv.*, 2014, **4**, 41956–41967; (*l*) K. Z. Elwakeel, G. O. El-Sayed and R. S. Darweesh, *Int. J. Miner. Process.*, 2013, **120**, 26–34; (*m*) K. Z. Elwakeel, M. A. Abd El-Ghaffar, S. M. El-kousy and H. G. El-Shorbagy, *Chem. Eng. J.*, 2012, **203**, 458–468; (*n*) D. Dontsova, S. Pronkin, M. Wehle, Z. Chen, C. Fettkenhauer, G. Clavel and M. Antonietti, *Chem. Mater.*, 2015, **27**, 5170–5179; (*o*) J. Zhang, L. A. Mitchell, D. A. Parrish and J. M. Shreeve, *J. Am. Chem. Soc.*, 2015, **137**, 10532–10535; (*p*) X. Qu, S. Zhang, Q. Yang, Z. Su, Q. Wei, G. Xie and S. Chen, *New J. Chem.*, 2015, **39**, 7849–7857; (*q*) G. Wang, T. Lu, G. Fan, C. Li, H. Yin and F. X. Chen, *Chem. – Asian J.*, 2018, **13**, 3718–3722; (*r*) L. Kukuljan and K. Kranjc, *Tetrahedron Lett.*, 2019, **60**, 207–209; (*s*) P. F. Pagoria, M.-X. Zhang, N. B. Zuckerman, A. J. DeHope and D. A. Parrish, *Chem. Heterocycl. Compd.*, 2017, **53**, 760–778.

19 V. N. M. de Oliveira, F. G. dos Santos, V. P. G. Ferreira, H. M. Araújo, C. do Ó Pessoa, R. Nicolete and R. N. de Oliveira, *Synth. Commun.*, 2018, **48**, 2522–2532.

20 (*a*) L. El Kaim, L. Grimaud and P. Patil, *Org. Lett.*, 2011, **13**, 1261–1263; (*b*) A. dos Santos, L. El Kaïm, L. Grimaud and C. Ronsseray, *Chem. Commun.*, 2009, 3907–3909; (*c*) H. X. Wang, T. Q. Wei, P. Xu, S. Y. Wang and S. J. Ji, *J. Org. Chem.*, 2018, **83**, 13491–13497; (*d*) T. H. Zhu, S. Y. Wang, Y. Q. Tao and S. J. Ji, *Org. Lett.*, 2015, **17**, 1974–1977; (*e*) C.-G. Liu, Z.-Y. Gu, H.-W. Bai, S.-Y. Wang and S.-J. Ji, *Org. Chem. Front.*, 2016, **3**, 1299–1303.

21 T. Soeta, A. Matsumoto, Y. Sakata and Y. Ukaji, *J. Org. Chem.*, 2017, **82**, 4930–4935.

22 (*a*) H. Yu, Y. Z. Li, Q. Liu, M. S. Zhang and W. L. Sun, *Chin. Chem. Lett.*, 2012, **23**, 130–132; (*b*) B. Mirza, *Tetrahedron Lett.*, 2016, **57**, 146–147.

23 A. P. Piccionello, A. Pace and S. Buscemi, *Chem. Heterocycl. Compd.*, 2017, **53**, 936–947.

24 (*a*) H. C. van der Plas, *Acc. Chem. Res.*, 1978, **11**, 462–468; (*b*) H. C. van der Plas, *Adv. Heterocycl. Chem.*, 1999, **74**, 1–253.

25 M. V. Il'in, A. S. Novikov and D. S. Bolotin, *J. Mol. Struct.*, 2019, **1176**, 759–765.
26 R. F. W. Bader, *Chem. Rev.*, 1991, **91**, 893–928.
27 (*a*) V. A. Dmitriev, M. M. Efremova, A. S. Novikov, V. V. Zarubaev, A. V. Slita, A. V. Galochkina, G. L. Starova, A. V. Ivanov and A. P. Molchanov, *Tetrahedron Lett.*, 2018, **59**, 2327–2331; (*b*) K. I. Kulish, A. S. Novikov, P. M. Tolstoy, D. S. Bolotin, N. A. Bokach, A. A. Zolotorev and V. Y. Kukushkin, *J. Mol. Struct.*, 2016, **1111**, 142–150.
28 (*a*) V. N. Mikhaylov, V. N. Sorokoumov, K. A. Korvinson, A. S. Novikov and I. A. Balova, *Organometallics*, 2016, **35**, 1684–1697; (*b*) A. G. Tskhovrebov, A. S. Novikov, O. V. Odintsova, V. N. Mikhaylov, V. N. Sorokoumov, T. V. Serebryanskaya and G. L. Starova, *J. Organomet. Chem.*, 2019, **886**, 71–75.
29 (*a*) T. V. Serebryanskaya, A. S. Novikov, P. V. Gushchin, M. Haukka, R. E. Asfin, P. M. Tolstoy and V. Y. Kukushkin, *Phys. Chem. Chem. Phys.*, 2016, **18**, 14104–14112; (*b*) A. A. Melekhova, A. S. Novikov, N. A. Bokach, M. S. Avdonceva and V. Y. Kukushkin, *Inorg. Chim. Acta*, 2016, **450**, 140–145.
30 (*a*) A. S. Novikov and M. L. Kuznetsov, *Inorg. Chim. Acta*, 2012, **380**, 78–89; (*b*) A. A. Melekhova, A. S. Smirnov, A. S. Novikov, T. L. Panikorovskii, N. A. Bokach and V. Y. Kukushkin, *ACS Omega*, 2017, **2**, 1380–1391.
31 T. Cardoso, O. Ribeiro, I. C. Aragao, A. Costa-Pereira and A. E. Sarmento, *BMC Infect. Dis.*, 2012, **12**, 375.
32 J. M. Llaca-Diaz, S. Mendoza-Olazaran, A. Camacho-Ortiz, S. Flores and E. Garza-Gonzalez, *Chemotherapy*, 2012, **58**, 475–481.
33 M. Vestergaard, D. Frees and H. Ingmer, *Microbiol. Spectrum*, 2019, **7**, 1–23.
34 M. Mioc, C. Soica, V. Bercean, S. Avram, M. Balan-Porcarasu, D. Coricovac, R. Ghiulai, D. Muntean, F. Andrica, C. Dehelean, D. A. Spandidos, A. M. Tsatsakis and L. Kurunczi, *Int. J. Oncol.*, 2017, **50**, 1175–1183.
35 (*a*) Y. Gao, L. X. Na, Z. Xu, S. Zhang, A. P. Wang, K. Lu, H. Y. Guo and M. L. Liu, *Chem. Biodiversity*, 2018, **15**, e1800261; (*b*) T. Plech, M. Wujec, U. Kosikowska, A. Malm, B. Rajtar and M. Polz-Dacewicz, *Eur. J. Med. Chem.*, 2013, **60**, 128–134.
36 D. Ding, M. A. Boudreau, E. Leemans, E. Spink, T. Yamaguchi, S. A. Testero, P. I. O'Daniel, E. Lastochkin, M. Chang and S. Mobashery, *Bioorg. Med. Chem. Lett.*, 2015, **25**, 4854–4857.
37 N. P. Rai, V. K. Narayanaswamy, T. Govender, B. K. Manuprasad, S. Shashikanth and P. N. Arunachalam, *Eur. J. Med. Chem.*, 2010, **45**, 2677–2682.
38 (*a*) L. Palatinus and G. Chapuis, *J. Appl. Crystallogr.*, 2007, **40**, 786–790; (*b*) L. Palatinus, S. J. Prathapa and S. van Smaalen, *J. Appl. Crystallogr.*, 2012, **45**, 575–580.
39 G. M. Sheldrick, *Acta Crystallogr., Sect. A: Found. Crystallogr.*, 2008, **64**, 112–122.
40 G. M. Sheldrick, *Acta Crystallogr., Sect. C: Struct. Chem.*, 2015, **71**, 3–8.
41 O. V. Dolomanov, L. J. Bourhis, R. J. Gildea, J. A. K. Howard and H. Puschmann, *J. Appl. Crystallogr.*, 2009, **42**, 339–341.
42 Y. Zhao and D. G. Truhlar, *Theor. Chem. Acc.*, 2007, **120**, 215–241.
43 M. J. Frisch, G. W. Trucks, H. B. Schlegel, G. E. Scuseria, M. A. Robb, J. R. Cheeseman, G. Scalmani, V. Barone, B. Mennucci, G. A. Petersson, H. Nakatsuji, M. Caricato, X. Li, H. P. Hratchian, A. F. Izmaylov, J. Bloino, G. Zheng, J. L. Sonnenberg, M. Hada, M. Ehara, K. Toyota, R. Fukuda, J. Hasegawa, M. Ishida, T. Nakajima, Y. Honda, O. Kitao, H. Nakai, T. Vreven, J. A. Montgomery Jr., J. E. Peralta, F. Ogliaro, M. Bearpark, J. J. Heyd, E. Brothers, K. N. Kudin, V. N. Staroverov, T. Keith, R. Kobayashi, J. Normand, K. Raghavachari, A. Rendell, J. C. Burant, S. S. Iyengar, J. Tomasi, M. Cossi, N. Rega, J. M. Millam, M. Klene, J. E. Knox, J. B. Cross, V. Bakken, C. Adamo, J. Jaramillo, R. Gomperts, R. E. Stratmann, O. Yazyev, A. J. Austin, R. Cammi, C. Pomelli, J. W. Ochterski, R. L. Martin, K. Morokuma, V. G. Zakrzewski, G. A. Voth, P. Salvador, J. J. Dannenberg, S. Dapprich, A. D. Daniels, O. Farkas, J. B. Foresman, J. V. Ortiz, J. Cioslowski and D. J. Fox, *Gaussian C.01*, 2010.
44 A. V. Marenich, C. J. Cramer and D. G. Truhlar, *J. Phys. Chem. B*, 2009, **113**, 6378–6396.
45 (*a*) C. Gonzalez and H. B. Schlegel, *J. Chem. Phys.*, 1989, **90**, 2154–2161; (*b*) C. Gonzalez and H. B. Schlegel, *J. Phys. Chem.*, 1990, **94**, 5523–5527; (*c*) C. Gonzalez and H. B. Schlegel, *J. Chem. Phys.*, 1991, **95**, 5853–5860.
46 T. Lu and F. Chen, *J. Comput. Chem.*, 2012, **33**, 580–592.
47 E. D. Glendening, C. R. Landis and F. Weinhold, *Wiley Interdiscip. Rev.: Comput. Mol. Sci.*, 2012, **2**, 1–42.
48 (*a*) R. Centore, C. Manfredi, A. Capobianco, S. Volino, M. V. Ferrara, A. Carella, S. Fusco and A. Peluso, *J. Org. Chem.*, 2017, **82**, 5155–5161; (*b*) T. Sergeieva, M. Bilichenko, S. Holodnyak, Y. V. Monaykina, S. I. Okovytyy, S. I. Kovalenko, E. Voronkov and J. Leszczynski, *J. Phys. Chem. A*, 2016, **120**, 10116–10122.

